

## Effect of Double-Atom Vacancy Defects on the Elastic Properties of Single-Layered Graphene Sheets

Z. Q. Wang, Z. W. Yu, X. Y. Sun,<sup>1</sup> H. Li, and Y. J. Wang<sup>2</sup>

College of Aerospace and Civil Engineering, Harbin Engineering University, Harbin, China

<sup>1</sup> sunxiaoyu520634@163.com

<sup>2</sup> 906871278@qq.com

УДК 539.4

## Влияние двойных атомарных вакансационных дефектов кристаллической решетки на упругие свойства однослойных листов графена

З. К. Ванг, З. В. Ю, К. Я. Сун, Х. Ли, И. Ж. Ванг

Колледж аэрокосмического и гражданского строительства, Харбинский инженерный университет, Харбин, Китай

В рамках подхода молекулярной структурной механики исследуется влияние двойных атомарных вакансационных дефектов кристаллической решетки на упругие свойства однослойных листов графена с зигзагообразной и плетеной структурой. Для моделирования межатомных сил связей типа углерод–углерод используется пространственная структурная сетка. Результаты численного моделирования, полученные методом конечных элементов, подтверждают, что наличие указанных вакансационных дефектов снижает модуль упругости графена, что приводит к уменьшению его несущей способности. Установлено, что увеличение количества вакансационных дефектов обуславливает снижение модуля упругости и коэффициента Пуассона однослойных листов графена.

**Ключевые слова:** графен, двойные атомарные вакансационные дефекты, упругие свойства, хиральность, молекулярная структурная механика.

**Introduction.** Graphene is a new type of low-dimensional carbon material, which emerged after the discovery of fullerenes and carbon nanotubes. Due to its single atomic layer thickness, graphene is considered to be a two-dimensional material, which consists of carbon atoms in a honeycomb lattice structure. Since its news-breaking appearance in 2004 [1], graphene has received significant attention due to its outstanding physical properties such as high thermal conductivity [2], stiffness, and strength [3]. However, the issue of mechanical properties of single-layered graphene sheets (SLGS) being impaired by atom vacancy defects has received scarce attention yet. However, due to limitations in the graphene production, imperfections, such as adatoms, Stone–Wales defects, line defects, and vacancies of atoms cannot be avoided in graphene nanostructures [4]. Of these, the vacancy defects are the most typical for graphene and strongly affect the mechanical properties of SLGS. Therefore, it is of high theoretical significance and practical importance to study the influence of double-atom vacancy defects (DAVD) on the mechanical properties of SLGS.

Numerous researchers have investigated the elastic properties of graphene using various theoretical methods. Thus, Pei et al. applied the molecular dynamics approach to estimate the elastic modulus values for different chirality graphenes, including the so-called

armchair and zigzag graphenes, for which the respective values of 0.89 and 0.83 TPa were reported in [5]. The application of another molecular dynamics method (namely, the empirical Tersoff potential) by Bu et al. [6] yielded the graphene elastic modulus of up to 1.24 TPa. Within framework of the ab initio density functional theory (via DFT method) Liu et al. [7] estimated the elastic modulus and Poisson's ratio of graphene as 1.05 TPa and 0.86, respectively. Also, Reddy adopted a continuum mechanics approach to determine the elastic modulus of non-equilibrium and equilibrium graphene, obtaining values of 1.0 and 0.7 TPa, respectively [8]. Li applied the structural mechanics approach to monolayer graphene, with the simulation of graphene sheets by space frame structures, and predicted that SLGS elastic modulus reaches 1.02 TPa [9]. However, there are scarce research reports on the effect of DAVDs on the elastic properties of SLGS.

A molecular structural mechanics approach was adopted in this paper to study the effect of DAVDs on the elastic properties of the zigzag and armchair SLGS with account of their sizes and the number of DAVDs.

**1. Theoretical Details.** In terms of the molecular mechanics, graphene as a large molecule contains many regularly arranged carbon atoms with each atom in a force field [9] that is generated by interactions between electron-nucleus and nucleus-nucleus and controls the atom movements. The steric potential energy corresponds to the force field, which controls only the relative location of the nuclei. In Fig. 1, different kinds of potential energy terms of carbon–carbon (C–C) bonds are illustrated.

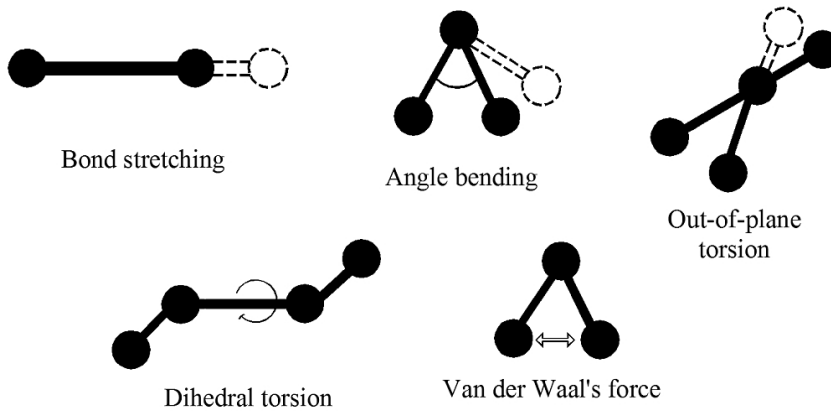


Fig. 1. Potential energy of C–C bonds.

For the system, the total potential energy functions are given by

$$U_{total} = \sum U_r + \sum U_\theta + \sum U_\phi + \sum U_\omega + \sum U_{vdw}, \quad (1)$$

where  $U_r$ ,  $U_\theta$ ,  $U_\phi$ ,  $U_\omega$ , and  $U_{vdw}$  are energies, related to the bond stretching, angle variation, inversion, angle variation, and van der Waals nonbonding interaction, respectively. The last term is negligible, in comparison with the other four terms that make the dominant contributions to the total steric energy. Furthermore, as compared to the other terms, the torsion and inversion energies are the most critical for the graphene subjected to in-plane tension loading. Consequently, the sum of angle variation and bond stretching terms, represented by harmonic functions under the assumption of small linearly elastic deformations, can be used to calculate the total energy of monolayer graphene with a fairly high accuracy [10–12]. The bond stretching and angle variation harmonic functions are derived via the following equations:

$$U_r = \frac{1}{2} k_r (r - r_0)^2 = \frac{1}{2} k_r (\Delta r)^2, \quad (2)$$

$$U_\theta = \frac{1}{2} k_\theta (\theta - \theta_0)^2 = \frac{1}{2} k_\theta (\Delta\theta)^2. \quad (3)$$

Here  $k_\theta$  and  $k_r$  represent the force constant for the angle variation and bond stretching, respectively,  $\theta$  and  $\theta_0$  are the bond angles after and before deformation, respectively, while  $r$  and  $r_0$  are the interatomic distances after and before the deformation, respectively.

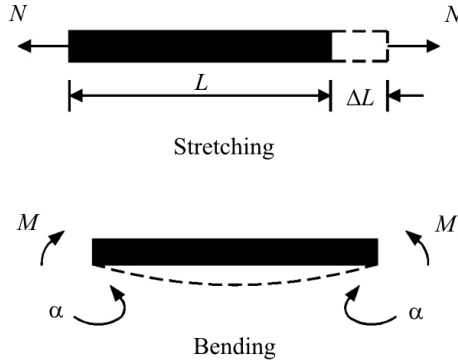


Fig. 2. Stretching and bending of a uniform beam.

Within framework of the structural mechanics, the beam potential energy can be expressed via twisting and stretching terms, which correspond to bending and tensile axial load schemes depicted in Fig. 2. Under the axial load  $N$ , a uniform beam's strain energy can be derived as

$$U_A = \frac{1}{2} \int_0^L \frac{N^2}{EA} dl = \frac{1}{2} \frac{N^2 L}{EA} = \frac{1}{2} \frac{EA}{L} (\Delta L)^2, \quad (4)$$

where  $U_A$  is tensile load energy,  $E$  is the elastic modulus of the uniform beam,  $A$  is the beam cross-sectional area,  $\Delta L$  is the elongation, and  $L$  is the length of beam. In case of application of a pure bending moment  $M$  (Fig. 2), the beam bending potential energy,  $U_M$ , is derived as follows:

$$U_M = \frac{1}{2} \int_0^L \frac{M^2}{EI} dl = \frac{2EI}{L} \alpha^2 = \frac{1}{2} \frac{EI}{L} (2\alpha)^2, \quad (5)$$

where  $\alpha$  is the rotation angle of the beam edges and  $I$  is the moment of inertia for this rotational motion.

That is to say, the equivalence of the relevant terms of molecular and structural mechanics systems is assumed due to the independence of their potential energy terms. This implies the equivalence of the molecular system and the structural beam, which is used to simulate the interatomic forces acting on the covalently bonded carbon atoms. The beam stiffness values correspond to the constants of covalent force field terms, which are derived as follows:

$$\frac{EA}{L} = k_r, \quad \frac{EI}{L} = k_\theta, \quad (6)$$

where  $k_r$  and  $k_\theta$  are the bending and stretching/tensile constants of the equivalent beams, respectively. These can be assessed by the stiffness matrix method. Alternatively, the structural beam simulation by atomistic finite elements was proposed [13].

It is noteworthy that specifying the diameter and elastic modulus of the beam allows one to compare the atomistic limited approach results with those of the stiffness matrix method. By substituting parameters  $A = \frac{\pi d^2}{4}$  and  $I = \frac{\pi d^4}{64}$  into Eq. (6), the beam characteristics can be derived via the force field constants as

$$d = 4\sqrt{\frac{k_\theta}{k_r}}, \quad E = \frac{k_r^2 L}{4\pi k_\theta}, \quad (7)$$

where  $E$  is the elastic modulus,  $d$  is the cross-sectional diameter, and  $L$  is the length of beam, which is assumed to be equal to the carbon covalent bond interatomic distance. Application of the AMBER force field of molecular dynamics simulation [12] yields  $k_\theta = 8.78 \cdot 10^{-10} \text{ N} \cdot \text{nm}/\text{rad}^2$  and  $k_r = 6.52 \cdot 10^{-7} \text{ N}/\text{nm}$ . The distance between two contiguous carbon atoms is estimated as 0.1412 nm [14]. Solving Eq. (7) yields  $E = 5.488 \cdot 10^{-6} \text{ N}/\text{nm}^2$  and  $d = 0.146618 \text{ nm}$ . Additionally, according to [15], Poisson's ratio  $\nu = 0.3$  is assumed.

To simulate the monolayer graphene nanofilms, the space frame structures, consisting of beam elements, are used in the theoretical analysis, which predicts that the mechanical characteristics of SLGS are size-dependent and exhibit a chirality. The latter refers to a property of asymmetry, due to which chiral objects are distinguishable from their mirror images. Figure 3 shows the chiral SLGS studied in this work, namely, zigzag and armchair sheets of different side width and length values, which are designated as  $b$  and  $a$ , respectively.

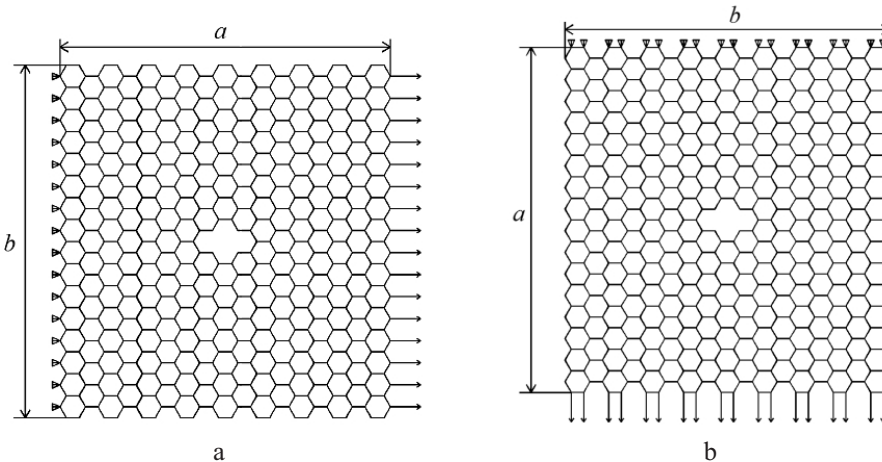


Fig. 3. Zigzag (a) and armchair (b) graphene with DAVDs.

To examine the elastic properties of the SLGS under study, a space frame structure model is used. The normal stress  $\sigma$  acting at the atomistic model's free edge is used for the exploration of the SLGS elastic properties under tension. As a result, the continuum sheet's normal stress is calculated as

$$\sigma = \frac{nf}{bt}, \quad (8)$$

where  $n$  is the number of nodes exposed to the external forces,  $f$  is the magnitude of the tensile forces,  $t$  and  $b$  are thickness and width of the SLGS, respectively. According to strain and tensile stress, the elastic modulus and Poisson's ratio are calculated as

$$E = \frac{\sigma}{\varepsilon_a} = \frac{nf}{\frac{\Delta a}{a}}, \quad \nu = \frac{\varepsilon_b}{\varepsilon_a} = \frac{\frac{\Delta b}{b}}{\frac{\Delta a}{a}}, \quad (9)$$

where  $\varepsilon_a$  and  $\varepsilon_b$  are tensile strains of SLGS, equal to the elongation ratios, while  $\Delta a$  and  $\Delta b$  are increments of the initial SLGS side length  $a$  and width  $b$ , respectively.

**2. Results and Discussion.** According to the theoretical analysis presented in the above section, the space frame structures consisting of beam elements are used to simulate the monolayer graphene nanofilms. To consider the influence of DAVDs on the elastic properties of SLGS with various sizes, the original model with seven sets of dimensions ( $a \times b$ ) was constructed: (a)  $0.985 \times 1.137$  nm, (b)  $1.969 \times 1.990$  nm, (c)  $2.953 \times 2.842$  nm, (d)  $3.938 \times 3.695$  nm, (e)  $4.430 \times 4.547$  nm, (f)  $5.415 \times 5.400$  nm, and (g)  $6.399 \times 6.252$  nm. The evolution of the elastic modulus and Poisson's ratios of zigzag and armchair SLGS with the increase in the number of DAVDs was also investigated in this study. It is considered that DAVDs located at the central line can eliminate the boundary effect of SLGS. The elastic moduli and Poisson's ratio of the zigzag and armchair SLGS were calculated for the above graphene sizes. These results are depicted in Figs. 4 and 5, respectively.

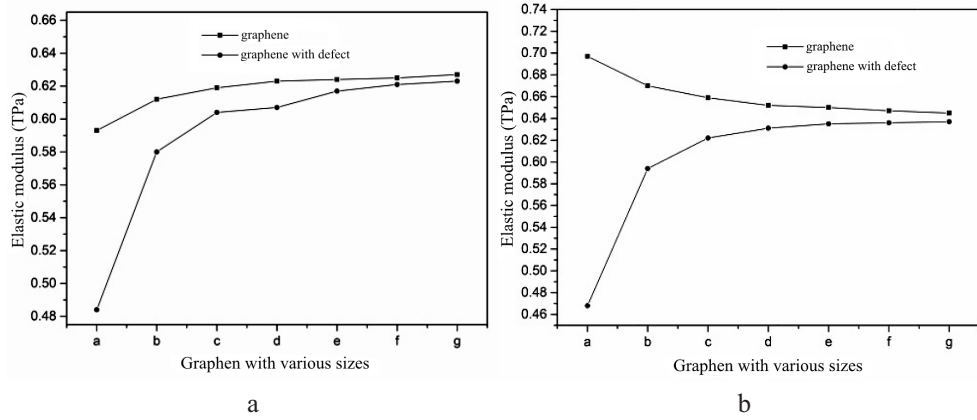


Fig. 4. The elastic modulus vs. size of zigzag (a) and armchair (b) SLGS.

**2.1. The Influence of DAVDs on the Elastic Properties of SLGS.** According to Figs. 4 and 5, the elastic moduli and Poisson's ratios of SLGS with DAVDs are lower than those of perfect SLGS, but with an increase in the SLGS size, this deterioration effect on the elastic properties is weakened, which finding proves that the elastic properties of SLGS are size-dependent. For the same size of graphene, the elastic modulus of zigzag SLGS is lower than that of armchair SLGS, which implies that the elastic properties of SLGS are also dependent on the chirality pattern.

For the dimensions of zigzag graphene with DAVDs, which correspond to the above cases (a)–(g) for, the respective reductions of Poisson's ratio and the elastic modulus corresponded to: (a) 9.96 and 8.38%, (b) 2.70 and 5.23%, (c) 1.02 and 2.42%, (d) 0.51 and 1.41%, (e) 0.50 and 0.96%, (f) 0.25 and 0.64%, and (g) 0.13 and 0.32%, respectively. For

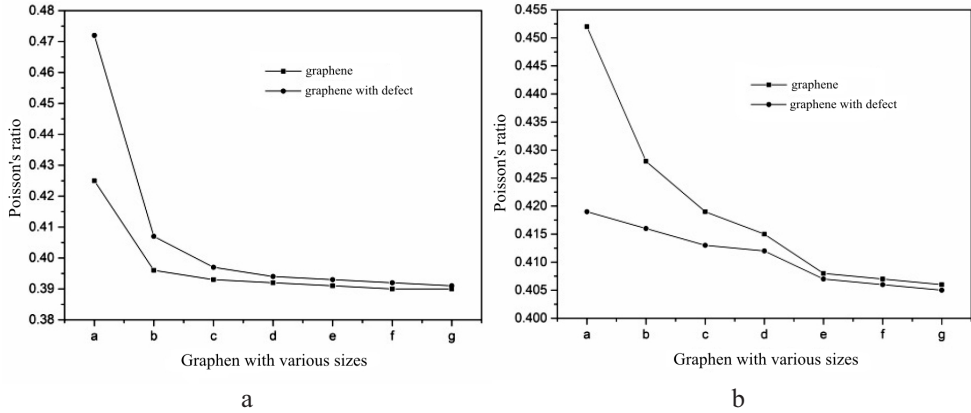


Fig. 5. Poisson's ratio vs. size of zigzag (a) and armchair (b) SLGS.

the armchair graphene, the respective reduction values were as follows: (a) 32.84 and 9.07%, (b) 11.34 and 2.80%, (c) 5.61 and 1.43%, (d) 3.22 and 0.72%, (e) 2.31 and 0.74%, (f) 1.71 and 0.49%, and (g) 1.05 and 0.24%. The above patterns depicted in Figs. 4 and 5 confirm that the effect DAVDs on the elastic properties of SLGS of two types of chirality weakens with their size. Moreover, the effect of DAVDs on the elastic properties of armchair SLGS is stronger than that on the zigzag one.

**2.2. Number of DAVDs vs. Elastic Properties.** The evolution of the elastic modulus and Poisson's ratios of zigzag and armchair SLGS with the increase in the number of DAVDs was also investigated in this study. For this purpose, the model of type ( $a \times b$ ) with the size of  $6.399 \times 6.252$  nm was constructed. DAVDs located at the central line are assumed to eliminate the boundary effect of SLGS. The elastic properties of zigzag and armchair SLGS with the number of DAVDs varying from zero to seven are depicted in Fig. 6, which demonstrates that the elastic modulus and Poisson's ratio of the armchair SLGS exceed those of the respective zigzag SLGS. In addition, an increase in the number of DAVDs leads to a continuous deterioration of the elastic properties of both types of SLGS. The deterioration of elastic properties of zigzag and armchair SLGS due to the availability of numerous DADS can be reduced to the elastic modulus decrease by 0.5 and 0.1% per defect, and that of Poisson's ratio by about 0.5 and 0.25% per defect, respectively.

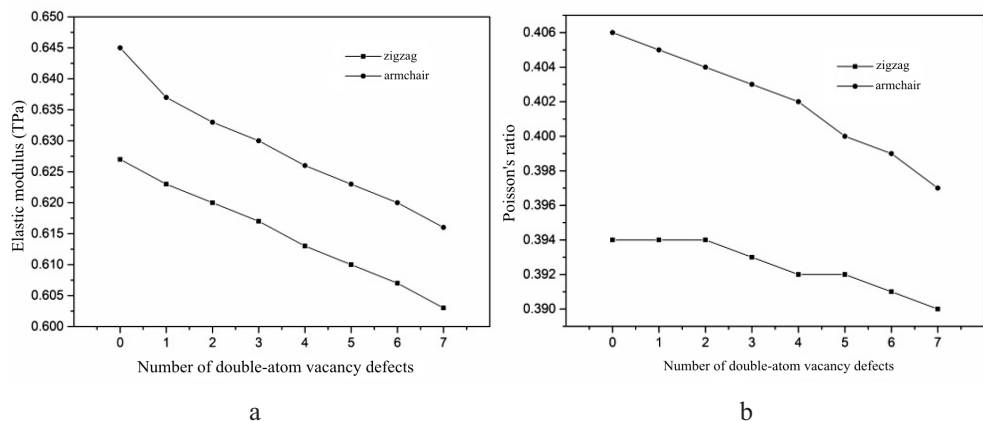


Fig. 6. Evolution of the elastic modulus (a) and Poisson's ratio (b) of SLGS for the number of DAVDs varying from zero to seven.

**Conclusions.** In this work, the molecular structural mechanics method was adopted to simulate the elastic properties of SLGS with DAVDs. The sizes of graphene sheets and the numbers of DAVDs were taken into account in the evaluation of the elastic moduli and Poisson's ratios of SLGS with two kinds of chiralities: zigzag and armchair ones. The results obtained show that the above parameters of the SLGS with DAVDs are lower than those of perfect SLGS. However, with increasing graphene size, the influence of DAVDs on the elastic properties of SLGS becomes weaker. DAVDs with the increasing graphene nanofilm size exert a stronger effect on the elastic properties of armchair SLGS, as compared to zigzag ones. For the constant graphene nanofilms' sizes, the increased amount of DAVDs leads to a continuous decline in the elastic moduli and Poisson's ratios of zigzag and armchair chirality SLGS.

**Acknowledgments.** This work was supported by the National Natural Science foundation of China (Nos. 11602066, 11472086, and 11532013) and the China Postdoctoral Science Foundation on the 56th batch of surface funds the project (2014M561327) and the National Science Foundation of Heilongjiang Province of China (QC2015058 and 42400621-1-15047), the Foundation Research Funds for the Central Universities.

### Резюме

У рамках підходу молекулярної структурної механіки досліджується вплив подвійних атомарних вакансійних дефектів кристалічної гратки на пружні властивості одношарових листів графена із зигзагоподібною та плетеною структурою. Для моделювання міжатомних сил зв'язків типу вуглець–вуглець використовується просторова структурна сітка. Результати чисельного моделювання, отримані методом скінченних елементів, підтверджують, що наявність указаних вакансійних дефектів знижує модуль пружності графена, що призводить до зменшення його несівної здатності. Установлено, що збільшення кількості вакансійних дефектів призводить до зниження модуля пружності та коефіцієнта Пуассона одношарових листів графена.

1. K. S. Novoselov, A. K. Geim, S. V. Morozov, et al., "Electric field effect in atomically thin carbon films," *Science*, **306**, No. 5696, 666–669 (2004).
2. A. P. Yu, P. Ramesh, M. E. Itkis, et al., "Graphite nanoplatelet-epoxy composite thermal interface materials," *J. Phys. Chem. C*, **111**, No. 21, 7565–7571 (2007).
3. C. Lee, X. D. Wei, J.W. Kysar, and J. Hone, "Measurement of the elastic properties and intrinsic strength of monolayer graphene," *Science*, **321**, No. 5887, 385–388 (2007).
4. F. Banhart, J. Kotakoski, and A. V. Krasheninnikov, "Structural defects in graphene," *ACS Nano*, **5**, No. 1, 26–41 (2011).
5. Q. X. Pei, Y. W. Zhang, and V. B. Shenoy, "A molecular dynamics study of the mechanical properties of hydrogen functionalized graphene," *Carbon*, **48**, No. 3, 898–904 (2010).
6. H. Bu, Y. F. Chen, M. Zou, et al., "Atomistic simulations of mechanical properties of graphene nanoribbons," *Phys. Lett. A*, **373**, No. 37, 3359–3362 (2009).
7. F. Liu, P. B. Ming, and J. Li, "Ab initio calculation of ideal strength and phonon instability of graphene under tension," *Phys. Rev. B*, **76**, No. 6, 064120-1–064120-7 (2007).
8. C. D. Reddy, S. Rajendran, and K. M. Liew, "Equilibrium configuration and continuum elastic properties of finite sized graphene," *Nanotechnology*, **17**, No. 3, 864–871 (2006).

9. C. Li and T. W. Chou, “A structural mechanics approach for the analysis of carbon nanotubes,” *Int. J. Solids Struct.*, **40**, No. 10, 2487–2499 (2003).
10. K. Machida, *Principles of Molecular Mechanics*, Kodansha and John Wiley & Sons Co-publication, Tokyo–New York (1999).
11. A. K. Rappe, C. J. Casewit, K. S. Colwell, et al., “UFF, a full periodic table force field for molecular mechanics and molecular dynamics simulations,” *J. Am. Chem. Soc.*, **114**, No. 25, 10024–10035 (1992).
12. W. D. Cornell, P. Cieplak, C. I. Bayly, et al., “A second generation force field for the simulation of proteins, nucleic acids, and organic molecules,” *J. Am. Chem. Soc.*, **117**, No. 19, 5179–5197 (1995).
13. G. M. Odegard, T. S. Gates, K. E. Wise, et al., “Constitutive modeling of nanotube-reinforced polymer composites,” *Compos. Sci. Technol.*, **63**, No. 11, 1671–1768 (2002).
14. M. S. Dresselhaus, G. Dresselhaus, and R. Saito, “Physics of carbon nanotubes,” *Carbon*, **33**, No. 7, 883–891 (1996).
15. H. Wan and F. Delale, “A structural mechanics approach for predicting the mechanical properties of carbon nanotubes,” *Meccanica*, **45**, No. 1, 43–51 (2010).

Received 14. 08. 2017